A NOx trap study using fast response emission analysers for model validation

Alimin, A.J. , Roberts, C.A. and Benjamin, S.F.

Published version deposited in CURVE January 2014

CURVE is the Institutional Repository for Coventry University
http://curve.coventry.ac.uk/open

2006-01-0685

A NO$_x$ Trap Study Using Fast Response Emission Analysers for Model Validation

A. J. Alimin, C. A. Roberts and S. F. Benjamin
Coventry University

**2006 SAE World Congress
Detroit, Michigan
April 3-6, 2006**

SAE *International*™

The Engineering Meetings Board has approved this paper for publication. It has successfully completed SAE's peer review process under the supervision of the session organizer. This process requires a minimum of three (3) reviews by industry experts.

For permission and licensing requests contact:

SAE Permissions
400 Commonwealth Drive
Warrendale, PA 15096-0001-USA
Email: permissions@sae.org
Tel: 724-772-4028
Fax: 724-776-3036

SAE®

Global Mobility Database®

All SAE papers, standards, and selected books are abstracted and indexed in the Global Mobility Database.

For multiple print copies contact:

SAE Customer Service
Tel: 877-606-7323 (inside USA and Canada)
Tel: 724-776-4970 (outside USA)
Fax: 724-776-0790
Email: CustomerService@sae.org

ISSN 0148-7191
Copyright © 2006 SAE International
Positions and opinions advanced in this paper are those of the author(s) and not necessarily those of SAE. The author is solely responsible for the content of the paper. A process is available by which discussions will be printed with the paper if it is published in SAE Transactions.

Persons wishing to submit papers to be considered for presentation or publication by SAE should send the manuscript or a 300 word abstract to Secretary, Engineering Meetings Board, SAE.

Printed in USA

2006-01-0685

A NO$_X$ Trap Study Using Fast Response Emission Analysers for Model Validation

A. J. Alimin, C. A. Roberts and S. F. Benjamin
Coventry University

ABSTRACT

Lean burn after treatment systems using NO$_X$ traps for reducing emissions from diesel exhausts require periodic regeneration after each storage stage. Optimising these events is a challenging problem and a model capable of simulating these processes would be highly desirable. This study describes an experimental investigation, which has been designed for the purpose of validating a NO$_X$ trapping and regenerating model. A commercial computational fluid dynamics (CFD) package is used, to model NO$_X$ trapping and regeneration, using the porous medium approach. This approach has proved successful for three way catalysis modelling. To validate the model a one-dimensional NOx trap system has been tested on a turbocharged, EGR cooled, direct injection diesel engine controlled with an engine management system via DSPACE. Fast response emission analysers have been used to provide high resolution data across the after-treatment system for model validation. Measurements show CO is the primary reductant. After the trap NO and NO$_2$ spikes (NO$_X$ slippage) were observed both at the beginning and end of the regeneration period. The former is believed to be due to insufficient reductant. Whilst the model can qualitatively describe the main storage and regeneration phases it failed to predict NO$_X$ slippage.

INTRODUCTION

In the UK, there has been a steady increase in the registration of diesel-powered vehicles, either for private or light goods categories [1]. It has been estimated that the number of registered diesel vehicles in 2004 has almost trebled from 1994, and 2004 saw an increase of over 2 million diesel-powered vehicles from 2001. Petrol-powered vehicles only increased by around 300,000 units for the same period. Details of the diesel-powered vehicles registered in UK, from the year 2001 until 2004, are shown in Table 1.

Table 1: Diesel-powered motor vehicles currently licensed: 2001 – 2004 [2]

Year	Diesel-powered vehicles
	body type cars (Thousands)
2001	3,459.5
2002	3,912.4
2003	4,399.6
2004	5,010.6

Diesel engines operate under lean conditions and reduction of NO$_X$ to N$_2$ is difficult due to the presence of excess O$_2$ in the exhaust stream [3]. Typically lambda is within 1.5-1.8 on full load and increases as the load reduces, with NO$_X$ generation related to the fuelling rate and engine load [4]. In general, ways of reducing NO$_X$ emissions are categorised into three main groups [5]:

- Development of systems to improve fuel mixture and combustion
- Use of alternative fuels or conventional fuels with additives
- Development and installation of new post-combustion treatment devices

NO$_X$ traps are currently under development for treating NO$_X$ emissions, as they have certain advantages over other diesel after-treatment devices, although they are sulphur sensitive [6, 7]. Periodic regeneration of the NO$_X$ trap under all driving condition is essential since the trap has a finite trapping capability. Regeneration also prolongs the durability of the trap [8].

NO$_X$ traps work by storing NO$_X$ emissions while the engine operates under lean conditions and are regenerated during a rich operating phase. This rapid switching between lean and rich conditions is challenging as far as engine management control and combustion processes are concerned. Fuel injection timing, throttling and the dilution rate of the EGR also influence the

storage and regeneration process. The ratio between lean and rich period is also influential and typical ranges are between 50-60s lean followed by 1-4s operation under rich conditions [9, 10]

An effective NO_X trap system demands optimisation of key engine operating parameters as part of the reduction process as insufficient reductants in the rich pulse will not completely reduce NO_X levels. Integrated control of exhaust gas recirculation (EGR) and turbocharging has been shown to result in a substantial reduction of NO_X emissions [11]. It has been reported that best desorption and reduction of NO_X is when the equivalence ratio, $\Phi=1.15$ ($\lambda=0.870$) when higher CO levels give shorter desorption times [12]. An addition of a diesel oxidation catalyst (DOC) prior to the trap will improve lean NO_X trap (LNT) performance, but will also give rise to an increase in fuel consumption (0.5%). The rich pulsing frequency and duration needs to vary with the operating conditions.

LNT technology is suitable for medium and heavy weight vehicles with flexible injection systems and could also be used together with diesel particulate filters (DPF), to achieve simultaneous reduction of both NO_X and PM emissions, where the LNT is usually placed after the DOC but before the DPF system. Furthermore, based on the general overview and expected emission control technologies that will be implemented in the coming years [13], it is expected that LNT will play an important part in curbing NO_X emissions, especially for the application in light-duty vehicles.

The current challenges facing the application of LNT catalysts are their lack of sulphur tolerance and the difficulty in achieving rich conditions. It has been claimed that the cost of NO_X trap systems for diesel after-treatment is much higher than other NO_X reduction systems such as selective catalytic reduction (SCR) [14] and so optimum design is critical. To this end a NO_X trap model is being developed and is to be validated against data obtained from a 1-D after-treatment system. The model and measurement programme are described in the following sections.

NO_X STORAGE AND REDUCTION

LNT catalysts are typically composed of a Pt-group metal, which plays an important role in the red-ox process and a basic adsorbent or base-metal-oxide (BMO) that is responsible for providing the storage capacity. This BMO can be an oxide or carbonate of alkali and alkaline earth elements. Typical BMOs are barium oxide (BaO) and barium carbonate ($BaCO_3$). The chemical reactions that occur on the LNT catalyst are very complex and involve the reaction of acidic gas (NO_2) with the BMO to form nitrate or nitroso-species on the surface of the catalyst, desorption of NO_X during purging and reduction with CO [3, 6, 15, 16, 17].

BASIS OF NO_X TRAP KINETIC MODELLING IN CFD

A simple chemical kinetic scheme has been described by Laurent et al. [17] to model NO_X storage. These authors discuss the initial formation of O^*, NO^* and NO_2^* where the * symbol indicates either that the radical is available on a Pt catalyst site or that a site is vacant. These very fast reactions are, however, not rate-determining for the functioning of the lean NO_X trap so the set of four reactions that describes NO_X storage under lean conditions is as below:
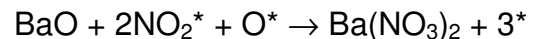
Rate R1 - NO oxidation under lean conditions

$$NO^* + O^* \rightarrow NO_2^* + *$$
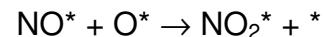
Rate R2 - The reverse reaction

$$NO_2^* + * \rightarrow NO^* + O^*$$
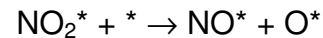
Rate R3 - NO_X trapping under lean conditions

$$BaO + 2NO_2^* + O^* \rightarrow Ba(NO_3)_2 + 3*$$

Rate R4 - Nitrate dissociation at high temperature

$$Ba(NO_3)_2 \rightarrow BaO + 2NO + 1.5O_2$$

The rates (mol/kg catalyst/s) for these reactions are given by Laurent et al. [17]. A full set of numerical values for rate constants is also available.

The porous medium or equivalent continuum approach is used in the CFD model described here. The CFD code STAR-CD was used for this study. The methodology is discussed elsewhere [18]. The 1D mesh is shown in Figure 1. The two separate smaller cell blocks model the bulk properties of the solid catalyst bricks for heat transfer from gas to wall and axial conduction in the substrate.
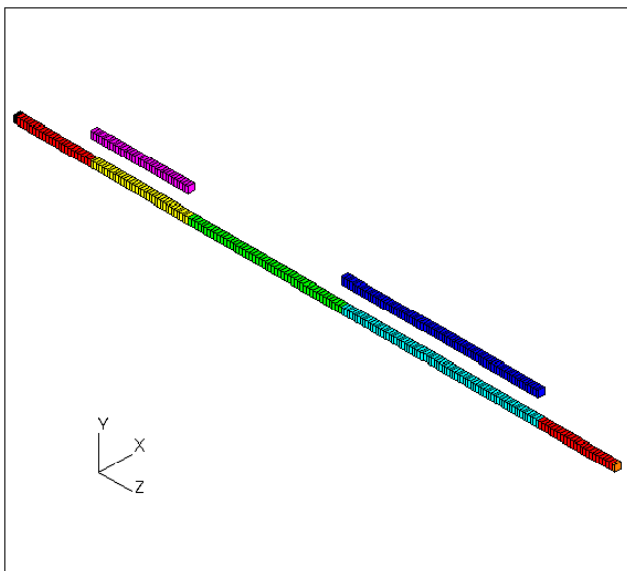
2

Figure 1: 1D mesh for NO$_X$ trap model showing fluid cell block with two porous medium sections that correspond to the separate solid cell blocks. Flow is in the +z direction. The shorter first brick is the DOC and the longer second brick is the NO$_X$ trap.

The modelling methodology requires that both the gas phase and solid phase species concentrations are properties of the porous fluid cells, since only the heat conduction equation with heat transfer source term is solved for the solid cells. The resistance of the porous medium to flow is described by the expression

$$\frac{\Delta P}{L} = -\alpha W_s^2 - \beta W_S \qquad (1)$$

where the permeability coefficient values α and β are temperature dependent. Upstream and downstream of the monolith the flow field is solved using the usual Reynolds averaged Navier Stokes methodology.

The solutions for both the solid phase and gas phase concentrations are obtained from the general conservation equation for chemical species, the transport equation, for which the 1D version is shown below.

$$\frac{\partial \rho C}{\partial t} + \frac{\partial (\rho W C)}{\partial z} - \frac{\partial}{\partial z}\left[\left[\frac{\mu_t}{\sigma_s} + \rho D\right]\frac{\partial C}{\partial z}\right] = Source\left(\frac{kg}{m^3/s}\right)$$

This equation has a transient term, a convective term, a diffusion flux term and a source term. The diffusion flux term applies within the fluid but the source term replaces it in the porous medium. An appropriate mass transfer coefficient from the thin film approximation is used to calculate the source term.

For the gas phase species in the porous medium, where the diffusion flux term is suppressed, the transport equation in 1D is written as equation (2) below.

$$\frac{\partial\left[\rho_{air} W_s C_{ig}\right]}{\partial z} + \varepsilon \rho_{air}\frac{\partial C_{ig}}{\partial t} = -K_{mi}\rho_{air}A_v\left[C_{ig} - C_{isol}\right]$$

$$(2)$$

Note that W_s is the superficial velocity for the porous medium such that $\rho_{air}W_s = \varepsilon\rho_{air}W$

For the solid phase species in the porous medium, the equation to be solved is

$$V_W\rho_{air}\left.\frac{\partial C}{\partial t}\right|_{isol} = K_m\rho_{air}A_V\left[C_{ig} - C_{isol}\right] + MR_i \qquad (3)$$

$$(kg/m^3 reactor/s)$$

where V_w indicates the fraction of the reactor volume available in the solid phase. Equation (3) has only transient and source terms; the other transport equation terms are suppressed within the CFD code.

The source terms for chemical species can be calculated using the expressions below within the CFD model.

Rate of NO reaction (kg NO /s /m^3 reactor) =

$$\frac{0.030}{V_w}\varepsilon\rho_c(R1 - R2 + 2R4) \qquad (4)$$

Rate of NO$_2$ reaction (kg NO$_2$ /s /m^3 reactor) =

$$\frac{0.046}{V_w}\varepsilon\rho_c(R1 - R2 - 2R3) \qquad (5)$$

Rate of O$_2$ reaction (kg O$_2$ /s /m^3 reactor) =

$$\frac{0.032}{V_w}\varepsilon\rho_c(0.5R2 - 0.5R1 - 0.5R3 + 1.5R4) \qquad (6)$$

The net rate of nitrate production is given below and the CFD solves equation (7) only for f, the value of the fraction.

$$\psi_{nitr\,ref}\frac{\partial f}{\partial t} = R3 - R4 \qquad (7)$$

The Laurent et al. scheme [17] is applied during the lean storage phases of the experiment. During regeneration, the storage scheme is switched off, the nitrate disintegrates and NO$_X$ is released. This is triggered by the local CO level in the model. The NO$_X$ is consumed in the model by, for example, the reaction with CO using

3

the kinetics of Siemund et al. [19] or by other appropriate reactions for which kinetics are available.

The reactions that occur in the first brick, the diesel oxidation catalyst (DOC), are oxidation of CO and hydrocarbons (HC) as occur in a 3-way catalyst, plus oxidation of NO to NO_2. These reactions are modelled in the porous medium cells that represent the DOC using the kinetic rate expressions identified by Triana et al. [20].

EXPERIMENTAL LAYOUT

For the experimental studies a 4-cylinder diesel engine was used equipped with a common rail injection system, EGR, VGT and an intake throttle body. The engine management system (ECU and ICU) and the throttle body are connected to the DSPACE control tool to enable the generation of the periodic rich combustion. Besides that, the engine management system is also connected to a GREDI system that is used as the calibration tool for the engine. Throughout the tests the engine used a very low sulphur diesel fuel, Carcal 55, Swedish Class Diesel, supplied by Petrochem. The engine specification is given in Table 2.

Table 2: Specification of the test engine

Items	Description
Engine capacity	1998 cc (86 mm bore, 86 mm stroke)
Rated power output	96 kW at 3800 rpm
Rated torque	330 N-m at 1800 rpm

The idealised after-treatment system was designed for model validation. It is a 1D system, which was developed in order to simplify model development. The turbo outlet of the engine is linked to a lean burn test rig that consists of a long diffuser followed by a flow straightener upstream of a DOC and an LNT. This ensures that the flow is approximately one-dimensional as in enters the DOC. The DOC uses Pt as the main catalytic compound whilst the LNT uses Pt and Rh as the reduction compounds. Figure 2 shows the layout for the experimental set-up and the details of the lean burn rig are illustrated in Figure 3.
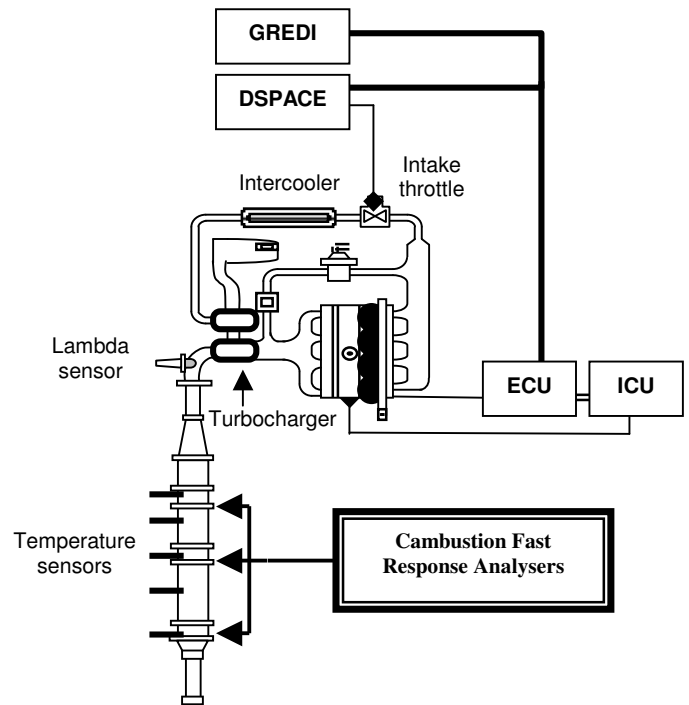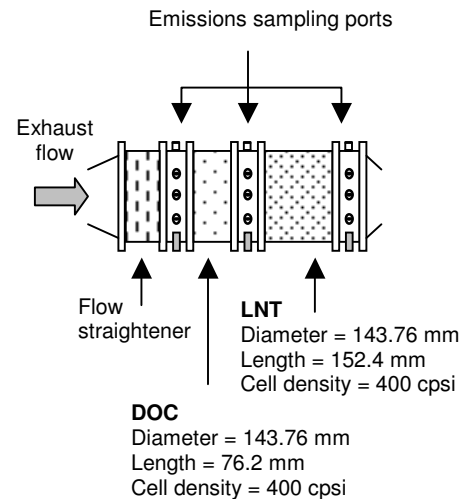

Figure 2: Schematic of the system set-up

Figure 3: Details of the Lean Burn Rig

The control algorithm set-up within the DSPACE system allows the control on the intake throttle body, EGR, VGT, as well as the injection quantities and timings for each of the Pilot, Main and Post injections. Besides that, it is also capable of producing different cyclic regeneration sets (alternating lean and rich operations), although it

4

only operates in open-loop. Cambustion fast response analysers are used to sample and analyse the exhaust emissions during storage and regeneration, with response time of less than 10 milliseconds. Data is logged at 60ms intervals. An HFR500 Fast FID (Flame Ionisation Detector) is used for sampling the HC emissions, an NDIR500 (Non-Dispersive Infra-Red) analyser is used for sampling the CO and CO2 and a CLD500 (Chemiluminescence) analyser is used to measure NO and total NO_X. The sampling probe without a NO_X converter is used to measure NO and with the converter to measure total NO_X, thus allowing for measurement of NO_2. Wide band lambda sensors were used to record air-fuel ratio.

The experiment was conducted under steady-state conditions, at an engine speed of 1500 rpm and a torque setting of 48 N-m. Emissions were sampled after the engine temperature and the catalyst bed temperatures had approximately stabilised. Temperatures were measured in front, within and after the DOC, inside the LNT and after the LNT. Three separate emission sampling positions were chosen: inlet (before the DOC), gap (between DOC and LNT) and exit (after the LNT). For the purpose of this study, the lean and rich durations were set at 60 seconds and 3 seconds respectively.

PERFORMANCE OF THE LNT DURING STORAGE AND REGENERATION EVENTS

Figure 4 shows a series of NO_X storage and purging cycles, which are repetitive and indicate the capability of the LNT system to reduce NO_X emissions. The regeneration events are indicated by the changes in the lambda values. Two NO_X spikes are generated at the beginning and end of purging and these are discussed later. Immediately after purging, NO_X emissions increased steadily before starting to stabilise after around 20 seconds, as the trap fills. As the total NO_X level in the gap in Figure 4 is less than the total NO_X at the inlet, reactions in the DOC could be generating N_2O.
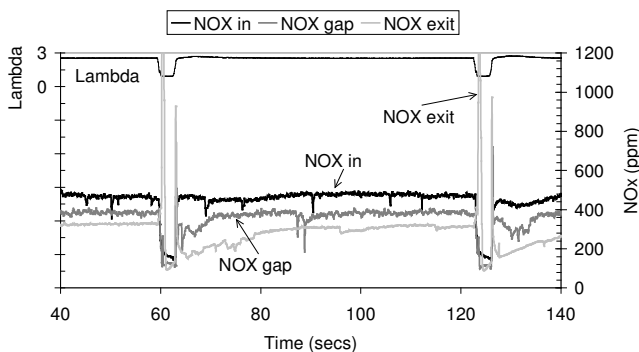

Figure 4: LNT storage and regeneration cycles (peaks NO_X at exit truncated)

Figure 5 shows the LNT efficiency, which is defined as below:

$$Efficiency = 100 \times \left[\frac{(NO_X)_{engine\_out} - (NO_X)_{downstream\_LNT}}{(NO_X)_{engine\_out}} \right]$$

The plot shows that as the storage period increases the efficiency drops as the trap fills up. Hence to maintain the LNT at high conversion efficiency, it is necessary to shorten the storage period and increase the purging frequency, or increase the purge duration. This LNT system operates with maximum efficiency of only around 65-70% and this implies that the implemented regeneration strategy can be improved further. The negative efficiencies are due to the NO_X spikes.
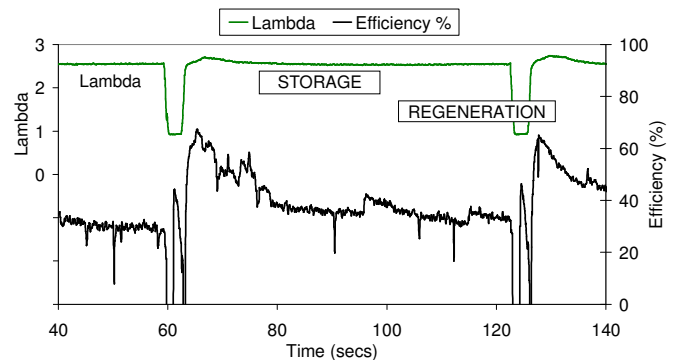

Figure 5: LNT efficiency

The individual plots for NO, NO_2, CO and HC during storage and regeneration are shown respectively in figures 6, 7, 8 and 9. The plots for NO, NO_2, CO and HC during regeneration for the sampling period 122 to 127 seconds, are depicted in figures 10, 11, 12 and 13. The plots from the temperature sensors placed at the inlet (before DOC), inside DOC and inside the LNT are shown in Figure 14.
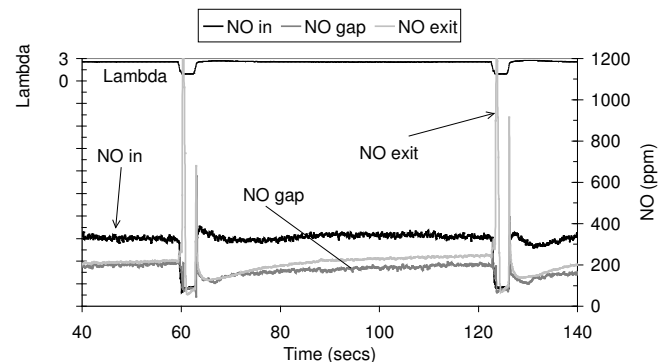

Figure 6: NO emissions during storage and regeneration (peaks NO at exit truncated)
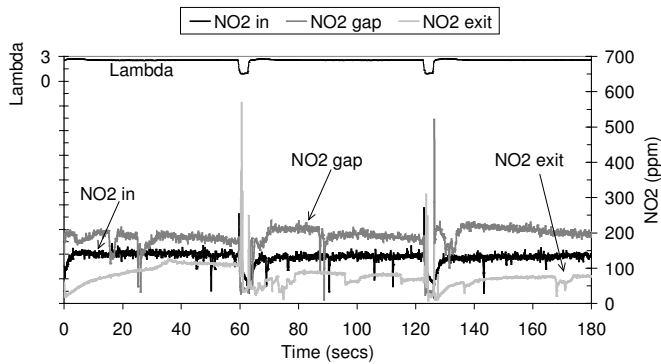
5

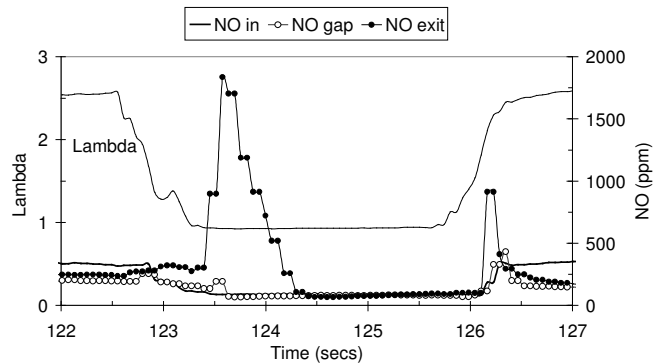Figure 7: NO_2 emissions during storage and regeneration

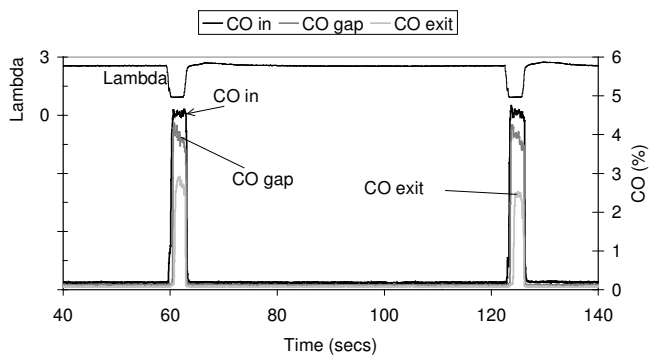Figure 10: NO emissions during regeneration
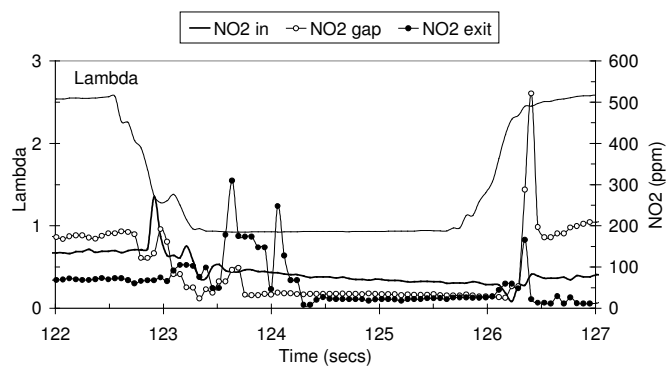

Figure 8: CO emissions during storage and regeneration

Figure 11: NO_2 emission during regeneration
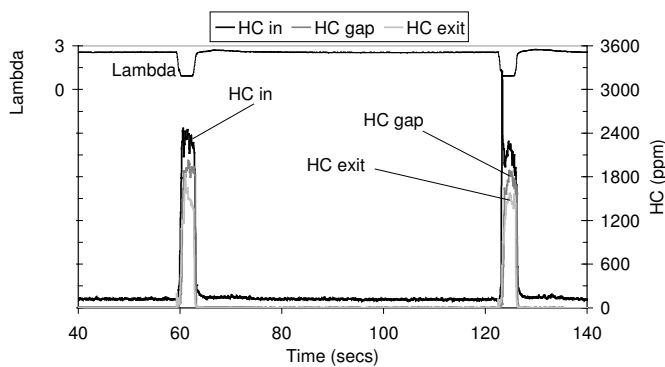

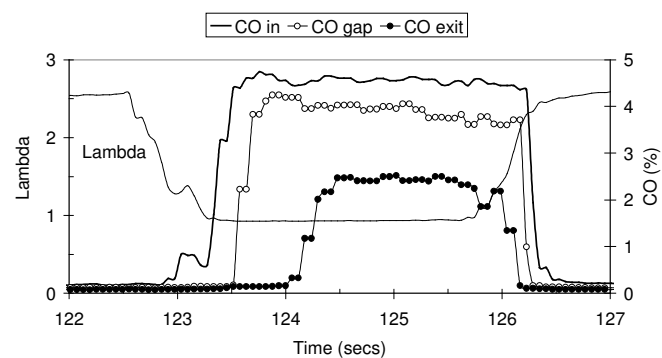Figure 9: HC emissions during storage and regeneration

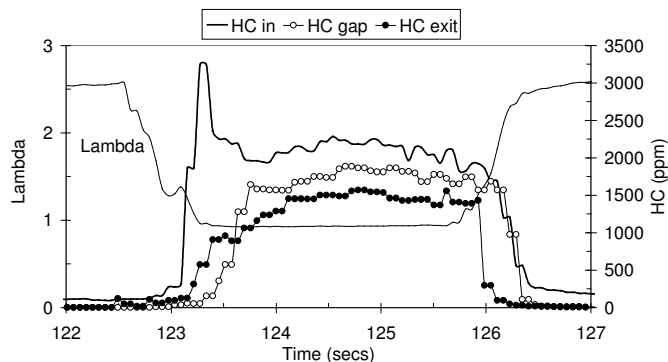Figure 12: CO emissions during regeneration
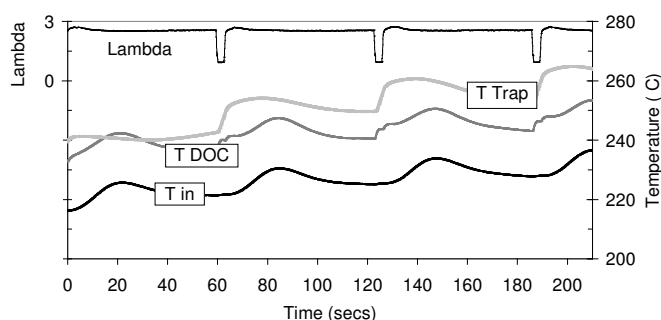
Figure 13: HC emissions during regeneration

Figure 14: Exhaust and catalysts bed temperatures during storage and regeneration

Figures 10 and 11 show that during regeneration (LNT purging), there are two very distinctive NO_X spikes observed after the LNT (NO_X slippage). The first NO_X release event occurs immediately into the regeneration stage (switching from the lean to rich) and the second event occurs at the end of the regeneration stage (switching from rich to lean). These spikes consist mainly of NO, rather than the NO_2 and are consistent throughout the storage and regeneration processes. The first spike peaked at 1835 ppm of NO and 245 ppm of NO_2, while the second spike peaked at 913 ppm of NO and 165 ppm of NO_2.

In Figure 10, the NO peak at the start and end of the regeneration originates in the NO_X trap. In Figure 11, the NO_2 peak at the end of the regeneration originates from the DOC and is inadequately stored by the trap during the changeover from rich to lean conditions.

Previous studies have also identified the presence of NO_X slip during regeneration [10, 21]. However, the NO_X spikes detected in this study during the rich duration are more well-defined. The study from Li et al. [10] shows NO_X slip only as a single peak. In the current study, the

use of fast response analysers has made it possible to detect the occurrence of two distinct NO_X spikes.

Li et al. [10] suggested that the occurrence of NO_X slip could be due to any of or a combination of factors: the long trapping duration, insufficient rich duration, the lambda value at LNT inlet being greater than 1, the LNT nearing its saturation point or the LNT bed temperature being either too high or too low. NO_X spikes observed in this study are probably due to insufficient reductant, as low CO levels are observed downstream of the LNT during the time when the first NO_X spike is observed.

For the HC emissions, lower levels are observed after the DOC and after the LNT, although they are not significantly different (Figure 9 & 13). Lower HC levels after the DOC are mainly due to the oxidation process inside the DOC.

CO emissions are much lower after the LNT than after the DOC as illustrated in Figure 12. Loss of CO emissions after the LNT indicates that the CO acts as the main or primary reductant for the purged NO_X. This is comparable to the findings from the study by West et al. [22].

MODELLING OF LNT DURING STORAGE AND REGENERATION

The CFD model described in this paper is very simple but it has numerous opportunities for tuning, and those that particularly affect the storage of NO_X and control the trap regeneration are:

The rate of NO to NO_2 conversion in DOC

The amount of catalyst on the NO_X trap, ρ_c

The rate of NO_X storage

The rate of disintegration of $Ba(NO_3)_2$

The rate of consumption by CO of NO released

Experimental data (Figs. 12 and 13) does suggest that CO is the main reducing agent and that hydrocarbon plays a smaller part in consumption of released NO, so the present model should describe the real situation by considering only consumption by CO.

Figures 15 and 16 below show predicted NO and NO_2 levels during storage and one regeneration event. The emission levels are predicted approximately correctly during storage, but during regeneration, consumption of the released NO by CO is complete and an NO spike is seen neither at the start nor the end of the regeneration.

Figure 17 shows the nitrate level predicted by the model and illustrates the storage and regeneration processes.

7

The NO spike at the start of regeneration (Fig. 10) can be displayed by the model, if the nitrate disintegration is triggered prior to the local rise in CO level. In reality, the regeneration must be triggered by the local change of the concentrations of chemical species within the NO_X trap. Since the O_2 level falls and the HC and CO levels rise simultaneously in the trap, it is difficult to envisage a mechanism that could trip the early release of NO to peak before sufficient CO is available.
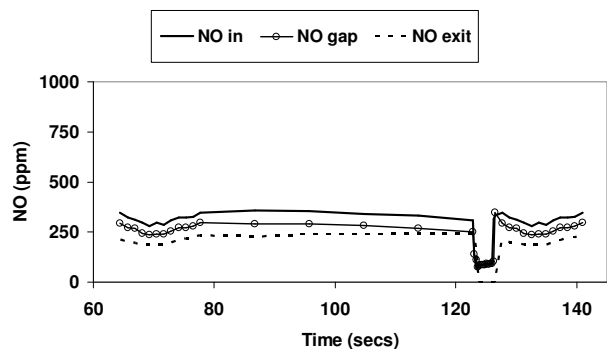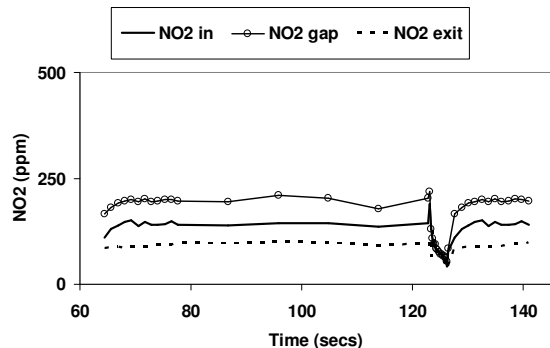

Figure 15: Predicted NO levels
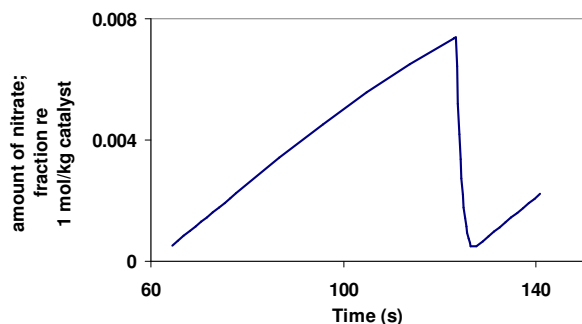

Figure 16: Predicted NO_2 levels

Figure 17: Predicted amount of nitrate at the mid point of the NO_X trap

The experimental data suggest that the initial rate of release of NO at the start of the regeneration is so fast that the available CO cannot consume it, but it has not yet been possible to reproduce this scenario with the present CFD model.

An advantage of the present model is its simplicity, and consequent low computational demand. It runs for about 80 seconds of real time in around 40 minutes on a single processor of an Itanium 2 under HP-UX.

Adding further reactions to the chemical scheme, for example a reaction of $Ba(NO_3)_2$ with CO to release NO_2 at regeneration and a reaction between CO and NO_2 to consume any NO_X released as NO_2 would add computational time without necessarily resolving the present problem that the NO slippage is not predicted.

CONCLUSION

In this study, a commercial CFD package is used to model the NO_X trap storage and regeneration, using the porous medium approach. Predictions are compared with measurements made with fast response emission analysers.

Experimental results show that CO acts as the primary reductant during the regeneration process. NO_X slip occurs as two events, at the beginning and end of regeneration and is dominated by the emissions of NO. The reason for the major NO_X slippage peak is due to insufficient reductant. The reasons for the second NO_X peak at the end of regeneration are unclear. An effective regeneration strategy is essential to deal with the NO_X slippage.

The model is shown to qualitatively describe the main storage and regeneration events but fails to predict NO_X slip. This is the subject of on-going research.

ACKNOWLEDGMENTS

REFERENCES

1. Department for Transport-DfT (2004) - *Vehicle Licensing Statistics 2003*, Transport Statistics Bulletin, available online, *www.dft.gov.uk*
2. Department for Transport-DfT (2005) - *Vehicle Licensing Statistics 2004*, Transport Statistics Bulletin, available online, *www.dft.gov.uk*
3. Epling, William S., Parks, James E., Campbell, Greg C., Yezerets, Aleksey, Currier, Neal W. and Campbell, Larry E. (2004) - *Further evidence of multiple NO_X sorption sites on NO_X storage/reduction*

8

catalysts, Catalysis Today, 96, (2004,) 21-30, www.elsevier.com/locate/cattod

4. Zheng, Ming; Reader, Graham T. and Hawley, J. Gary (2004) - *Diesel engine exhaust gas recirculation – a review on advanced and novel concepts*, Energy Conversion and Management, Volume 45, Issue 6, April 2004, pg 883-900

5. Armas, O; Baltesteros, R; Martos, F.S. and Agudelo, J.R. (2004) - *Characterization of light duty Diesel engine pollutant emissions using water-emulsified fuel*, Fuel, Vol. 84, Number 7-8, available online 15 December 2004, www.sciencedirect.com

6. Fang, Howard L.; Huang, Shyan C.; Yu, Robert C., Wan, C.Z. and Howden, Ken (2002) - *A Fundamental Consideration on NO_X Adsorber Technology for DI Diesel Application*, SAE2002-01-2889, Powertrain and Fluid Systems, Conference and Exhibition, San Diego, California, USA, 21-24th October 2002

7. West, Brian H. and Sluder, C. Scott (2000) - *NO_X Adsorber Performance in A Light-Duty Diesel Vehicle*, SAE2000-01-2912, International Fall Fuels and Lubricants, Meeting and Exposition, Baltimore, Maryland, October 16-19, 2000

8. Guyon, M.; Blanche P.; Bert, C.; Phillippe, L. and Messaoudi, I. (2000) - *NO_X-Trap System Development and Characterization for Diesel Engines Emission Control*, SAE 2000-01-2910, SAE International Fall Fuels and Lubricants, Meeting and Exhibition, Baltimore, USA, Oct 16-19, 2000

9. Nakatani, Koichiro; Hirota, Shinya; Takeshima, Shinichi; Itoh, Kazuhiro; Tanaka, Toshiaki and Dohmae, Kazuhiko (2002) - *Simultaneous PM and NO_X Reduction System for Diesel Engines*, SAE2002-01-0957, Diesel Exhaust Emissions Control, SAE 2002 World Congress Detroit, Michigan, March 4-7, 2002

10. Li, Yuejin; Roth, Stan, Yassine, Mahmoud, Beutel, Tilman, Dettling, Joe and Sammer, Chris (2000) - *Study of Factors Influencing the Performance of A NO_X Trap in a Light-Duty Diesel Vehicle*, SAE2000-01-2911, SAE International Fall Fuels and Lubricants, Meeting and Exhibition, Baltimore, USA, Oct 16-19, 2000

11. Capobianco, M. (2001) - *Optimum Control of an Automotive Direct Injection Diesel Engine for Low Exhaust Emissions*, Proc. Inst. Mech. Engineers-Part D, Journal of Automobile Engineering, Volume 215, 2001

12. Johnson, Timothy V. (2002) - *Diesel Emission Control: 2001 in Review*, SAE2002-01-0285, SAE 2002 World Congress, Detroit, Michigan, March 4-7, 2002

13. Johnson, Timothy V. (2003) - *Diesel Emission Control in Review-The Last 12 Months*, SAE2003-01-0039, 2003 SAE World Congress, Detroit, Michigan, March 2-3, 2003

14. Warren, James P. (2001) - *Diesel Aftertreatment Systems: 2004-2007, A Cost Assessment*, SAE2001-01-1948, International Spring Fuels and Lubricants, Meeting and Exhibition, Orlando, Florida, May 7-9, 2001

15. Touns, Mourad; Menegazzi, Pascal and Rouchon, Pierre (2003) - *NO_X Trap Model for Lean Burn Engine Control,* SAE2003-01-2292, 2003, Advanced Diesel Engines and Liquid Alternative Fuels, Future Transportation Technology Conference, Costa Mesta, California, June 23-25, 2003

16. Ketfi-Cherif, Ahmad; Wissel, Dirk von; Beurthey, Stephen and Sorine, Michel (2000) - *Modelling and control of a NO_X trap catalyst,* SAE2000-01-1199, 2000 SAE World Congress, Detroit Michigan, March 6-9, 2000

17. Laurent, F., Pope, C. J., Mahzoul, L., Delfosse, L., Gilot, P. (2003) - *Modelling of NO_X adsorption over NOx adsorbers*, Chem Eng Sci, Vol. 58 (2003) pp 1793-1803

18. S. F. Benjamin, C. A. Roberts. (2005) - *3D modelling of NO_X and particulate traps using CFD: a porous medium approach.* Submission to Applied Mathematical Modelling, 2005-09-28

19. Siemund, S., Lecelrc, J. P., Schweich, D., Prigent, M., Castagna, F. (1996) - *Three way monolithic converter: simulations versus experiments.* Chem Eng Sci , Vol. 51 No. 15 (1996) pp 3709 - 3720

20. Triana, Antonio P.; Johnson, John H.; Yang, Song L. and Baumgard, Kirby J. (2003) - An Experimental and Numerical Study of the Performance Characteristics of the Diesel Oxidation Catalyst in a Continuously Regenerating Particulate Filter, SAE2003-01-3176.

21. Sluder, C. Scott and West, Brian H. (2002) - *Effects of Regeneration Conditions on NO_X Adsorber Performance*, SAE2002-01-2876, Powertrain and Fluid Systems, Conference and Exhibition, San Diego, California, USA, October 21-24, 2002

22. West, Brian; Huff, Shean; Parks, James; Lewis, Sam; Choi, Jae-Soon; Partridge, William and Storey, John (2004) - *Assessing Reductant Chemistry During In-Cylinder Regeneration of Diesel Lean NO_X Traps*, SAE2004-01-3023, Powertrain and Fluid Systems Conference and Exhibition, Tampa, Florida USA, October 25-28, 2004.

CONTACT

Prof S. F. Benjamin, Centre for Automotive Engineering Research and Technology (CAERT), Faculty of Engineering and Computing, Coventry University, Priory Street, Coventry CV1 5FB.

Email: s.benjamin@coventry.ac.uk

μ_t	-	Turbulent dynamic viscosity (kg/(m s))

DEFINITIONS AND NOMENCLATURE

	ρ	-	Density (kg/m^3)

DOC	-	Diesel Oxidation Catalyst
LNT	-	Lean NO$_X$ Trap
ECU	-	Engine Control Unit
ICU	-	Injection Control Unit
EGR	-	Exhaust Gas Re-circulation
VGT	-	Variable Geometry Turbine
A_v	-	Reactor surface per unit reactor volume (m^2/m^3)
C	-	Mass fraction
$C_{i\,g}$	-	Species i mass fraction in the gas phase
$C_{i\,sol}$	-	Species i mass fraction in the solid phase
D	-	Species diffusivity (m^2/s)
f	-	Factor, fraction < 1
K_{mi}	-	Mass transfer coefficient (m/s)
L	-	Substrate length (m)
M	-	[kg /mol] for species i
ΔP	-	Pressure drop (Pa)
R_i	-	net rate of production of species i by reactions (mol /s /m^3 reactor)
Rn	-	Reaction rate for equation n
t	-	Time (s)
T	-	Temperature (K)
V_w	-	Volume in solid phase (pore volume) per unit volume of reactor [m^3 /m^3 reactor]
W	-	Velocity in the axial direction (m/s)
W_s	-	Superficial velocity, εW(m/s)
z	-	Axial coordinate
ε	-	Porosity of the substrate expressed as a volume fraction
λ	-	Lambda ratio
φ	-	Equivalence ratio

ρ_c	-	Catalyst loading (kg cat /m^3 reactor)
σ_s	-	Turbulent Schmidt No.
$\Psi_{nitr\,ref}$	-	Reference amount of Barium Nitrate (mol of nitrate/ kg cat.)

10